Published in final edited form as:
Bone. 2013 August ; 55(2): 449–457. doi:10.1016/j.bone.2013.02.023.

PTH prevents the adverse effects of focal radiation on bone architecture in young rats

Abhishek Chandra[1], **Shenghui Lan**[1,^], **Ji Zhu**[1], **Tiao Lin**[1], **Xianrong Zhang**[1,*], **Valerie A. Siclari**[1], **Allison R. Altman**[1], **Keith A. Cengel**[2], **X. Sherry Liu**[1], and **Ling Qin**[1,#]

Abhishek Chandra: abhic@mail.med.upenn.edu; Shenghui Lan: ocean.blue7@qq.com; Ji Zhu: zhuji@mail.med.upenn.edu; Tiao Lin: lintiao11@163.com; Xianrong Zhang: xianrongzh@yahoo.com; Valerie A. Siclari: vsiclari@mail.med.upenn.edu; Allison R. Altman: alaltman@mail.med.upenn.edu; Keith A. Cengel: keith.cengel@uphs.upenn.edu; X. Sherry Liu: xiaoweil@mail.med.upenn.edu

[1]Department of Orthopaedic Surgery, University of Pennsylvania, Philadelphia, Pennsylvania, USA

[2]Department of Radiation Oncology, Perelman School of Medicine, University of Pennsylvania, Philadelphia, Pennsylvania, USA

Abstract

Radiation therapy is a common treatment regimen for cancer patients. However, its adverse effects on the neighboring bone could lead to fractures with a great impact on quality of life. The underlying mechanism is still elusive and there is no preventive or curative solution for this bone loss. Parathyroid hormone (PTH) is a current therapy for osteoporosis that has potent anabolic effects on bone. In this study, we found that focal radiation from frequent scans of the right tibiae in 1-month-old rats by micro-computed tomography severely decreased trabecular bone mass and deteriorated bone structure. Interestingly, PTH daily injections remarkably improved trabecular bone in the radiated tibiae with increases in trabecular number, thickness, connectivity, structure model index and stiffness, and a decrease in trabecular separation. Histomorphometric analysis revealed that radiation mainly decreased the number of osteoblasts and impaired their mineralization activity but had little effects on osteoclasts. PTH reversed these adverse effects and greatly increased bone formation to a similar level in both radiated and non-radiated bones. Furthermore, PTH protects bone marrow mesenchymal stem cells from radiation-induced damage, including a decrease in number and an increase in adipogenic differentiation. While radiation generated the same amount of free radicals in the bone marrow of vehicle-treated and PTH-treated animals, the percentage of apoptotic bone marrow cells was significantly attenuated in the PTH group. Taken together, our data demonstrate a radioprotective effect of PTH on bone structure and bone marrow and shed new light on a possible clinical application of anabolic treatment in radiotherapy.

[#]Correspondence: Ling Qin, Ph.D., 424D Stemmler Hall, 36th Street and Hamilton Walk, Philadelphia, PA 19104. Tel: 215-8986697; Fax: 215-5732133; qinling@mail.med.upenn.edu.
[^]Present address: Department of Orthopaedic Surgery, Wuhan General Hospital of Guangzhou Military Command, Hubei Province, People's Republic of China
[*]Present address: Department of Physiology, School of Basic Medical Sciences, Wuhan University, Hubei Province, People's Republic of China

Disclosures: all authors state that they have no conflicts of interests.

Keywords

radiation therapy; μCT; PTH; trabecular bone; osteoblasts

Introduction

Ionizing radiation therapy, also known as radiotherapy, is used in the treatment of patients with malignant tumors due to its ability to induce cancer cell cytotoxicity. Approximately two-thirds of patients with solid malignancies (i.e. breast, prostate, cervical, lung, head and neck cancers, and soft tissue sarcoma) receive radiotherapy as a part of their treatment course. While current technologies allow unprecedented precision in radiotherapy delivery that spares most normal tissues, it is inevitable that some normal tissues will receive a significant radiation dose during treatment. Bone is one of the most commonly irradiated normal tissues and irradiation of bone can lead to multiple morbidities including fracture and loss of marrow function. While the rates of fracture depend on the radiation dose and the specific bone involved, increased fracture risk is a significant side effect of radiotherapy, especially in patients with thoracic and pelvic malignancies. For example, radiation-associated rib fracture rates in breast cancer patients range from 1.8% to 19% [1, 2]. A retrospective analysis of more than 6,000 post-menopausal women receiving radiotherapy for cervical, rectal, and anal cancers revealed as much as a 3-fold increase in hip fractures after radiation [3]. A study of 45,662 prostate cancer patients found that external beam radiotherapy significantly increases the risk of hip fractures by 76% [4]. Many cancer patients receiving radiotherapy are elderly and already at greatest risk of osteoporotic fractures and pelvic fractures are a major source of morbidity and mortality in this population [5–7]. Radiation-related fractures of hip and other pelvic bones, such as the sacrum, are associated with high morbidity and significant mortality since these fractures have very high rates of delayed union and nonunion. Surgical treatment with internal fixation and conventional bone grafting has only limited success [8]. To date, there is no preventive or curative treatment for radiation-induced bone damage. Because radiotherapy greatly improves survivorship rate and overall quality of life of cancer patients, it is thus imperative to investigate the mechanisms of radiation on the skeletal system and to identify a treatment to reverse its damage to bone.

The detrimental effects of radiation on the skeletal system have also been demonstrated in rodent models. Recent studies [9–12] demonstrated that radiation on mice resulted in a marked decrease in trabecular bone volume fraction starting from 2 weeks and persisted over 2–3 months post-irradiation. Bone histomorphometry and serum chemistry analyses suggested that decreased osteoblast activity and increased osteoclast activity are the most likely causes of this bone loss [9, 12]. In addition, radiation exposure leads to reduced marrow cellularity [13] and a rapid collapse of bone marrow cells, including hematopoietic stem cells (HSCs) and hematopoietic subpopulations [9]. Interestingly, an abscopal (distant) effect of bone loss in long bones was observed in mice receiving abdominal irradiation [14]. However, in contrast to the localized radiation used in the clinic for most cancer patients, all of these studies exposed either the entire or a large portion of animal body to the radiation. Therefore, their conclusions cannot exclude the possible systemic effects of radiation, which are evident from the altered body and organ (thymus and spleen) weights observed in these reports [9, 13, 14].

Parathyroid hormone (PTH) is a major endocrine regulator of calcium and phosphorus homeostasis and current interests in PTH focus on its potent anabolic action on bone. Recombinant human PTH(1–34), marketed as Forteo, was approved by the FDA in 2002 for the treatment of osteoporosis in postmenopausal women and men who are at a high risk for

fracture. Intermittent PTH injections greatly stimulate bone turnover, namely bone formation and resorption, with a greater effect on formation than resorption, leading to a net bone gain [15]. PTH exerts most of its effects on trabecular bone with dramatic increases in bone volume, connectivity and plate-like microarchitecture [16, 17]. Multiple mechanisms, including activating bone lining cells, stimulating osteoblast differentiation, preventing osteoblast apoptosis, and enhancing bone resorption, have been proposed to mediate this anabolic effect [18, 19]. In the past, we showed that PTH, acting through its receptor PTH1R in osteoblasts, profoundly regulates gene expression profiles in osteoblastic cultures [20] and rat trabecular bone [21]. These PTH-regulated genes (growth factors, signal transducers, structural molecules, transcription factors, transporters, and enzymes etc) have broad functions, implying that PTH influences many biological processes in osteoblasts and their bone marrow environment.

In this study, we attempt to determine whether PTH could be used in radiotherapy to protect bone from radiation-induced bone damage. We first set up a focal radiation animal model using high-resolution micro-computed tomography (μCT). We found that, while frequent μCT scans of the tibial trabecular region of young rats caused severe bone loss and bone structural deterioration specifically within the scanned area, daily injections of PTH for the duration of scanning not only prevented the μCT radiation-induced bone loss but greatly improved the bone microachitecture. Three-dimensional analyses of μCT images, bone histomorphometry, and analyzing bone marrow cells were performed to understand the underlying mechanisms.

Material and Methods

Rat study design

All animal studies performed in this report were reviewed and approved by the Institutional Animal Care and Use Committee (IACUC) at the University of Pennsylvania. One-month-old male Sprague Dawley rats (Charles River, Wilmington, MA) were given food and water ad libitum. Rats were divided into the following three groups with similar body weight at the outset of the study. Groups A and B (n=8/group) received vehicle and human recombinant PTH(1–34, 80 μg/kg/day, Bachem, Switzerland), respectively, daily from day 0 to 11. Both groups received μCT scans on the right tibiae every other day from day 0 to 10. On day 12, both left and right tibiae were scanned. Right tibiae were considered as radiated and left tibiae as non-radiated. They were injected subcutaneously with 15 mg/kg calcein (Sigma Aldrich, St. Louis, MO) at day 3 and 10 for dynamic histomorphometric measurements. Group C (n=6), serving as non-radiated controls, received isoflurane anesthesia (4% induction and 1.5% maintenance) with right tibiae stabilized in a customized holder for 20 min (the approximate μCT scanning time) once every other day from day 0 to 10 and saline (vehicle) injection daily from day 0 to 11. On day 12, both left and right tibiae were scanned by μCT. Animals were euthanized on day 12 after the last μCT scan and tissues, such as tibiae, blood, thymus, and spleen, were harvested for analysis.

In vivo micro-computed tomography

Each rat was anesthetized by isoflurane (4% induction and 1.5% maintenance) and its right or left tibia was secured by a customized holder to ensure minimal motion effect before the rat was inserted into the scanning chamber of an in vivo μCT system (VivaCT 40, Scanco Medical AG, Switzerland). A scout view of the entire tibia was first performed to measure the length of the tibia from the upper extremity to the lower extremity. Then the proximal end of the tibia, corresponding to a 0–4.4 mm region below the lowest point of growth plate, was scanned at 10.5 μm isotropic voxel size to acquire a total of 417 slides. All images were first smoothed by a Gaussian filter (sigma=1.2, support=2.0) and then thresholded

corresponding to 27% (trabecular bone) and 36% (cortical bone) of the maximum available range of image grayscale values. The images of the secondary spongiosa regions 2.5–4.0 mm and 3.1–3.6 mm below the lowest point of growth plate were contoured for trabecular and cortical bones, respectively. Trabecular volumetric bone mineral density (vBMD), bone volume fraction (BV/TV), trabecular thickness (Tb.Th*), trabecular separation (Tb.Sp*), trabecular number (Tb.N*), structure model index (SMI), connectivity density (Conn.D), cortical BMD, periosteal perimeter (Ps.Pm), endocortical perimeter (Ec.Pm), cortical area (Ct.Ar), cortical bone thickness (Ct.Th), and moment of inertia (MOI) were calculated by 3D standard microstructural analysis [22].

Based on thresholded whole bone images, microstructural finite element (μFE) models were generated by converting each bone voxel to an 8-node brick element. Bone tissue was modeled as an isotropic, linear elastic material with a Young's modulus of 15 GPa and a Poisson's ratio of 0.3. A uniaxial compression was applied along the axial direction of the model and the model was subjected to a linear elastic analysis to determine bone stiffness.

Static and dynamic histomorphometry

Both left and right tibiae from groups A and B were dissected and processed for methylmethacrylate embedding. Five μm longitudinal sections were cut using a Polycut-S motorized microtome (Reichert, Heidelberg, Germany) and stained with Goldner's trichrome stain. Unstained 8 μm sections were used for dynamic measurements. All histomorphometric measurements were performed in an area 2.0–5.2 mm below the growth plate using Bioquant Osteo Software (Bioquant Image Analysis, Nashville, TN). The primary indices include the total tissue area (TV), trabecular bone perimeter (BS), trabecular bone area (BV), osteoblast surface (Ob.S), osteoblast number (Ob.N), osteoclast surface (Oc.S), single- and double-labeled surface, and interlabel width. The percentage of osteoblast surface (Ob.S/BS), osteoblast number (Ob.N/BS), osteoclast surface (Oc.S/BS), and mineralizing surface (MS/BS), mineral apposition rate (MAR, μm/day), and surface-referent bone formation rate (BFR/BS, $\mu m^3/\mu m^2$/day) were calculated as described by Parfitt et al. [23].

Serum chemistry

Blood was collected from cardiac puncture at the time of euthanization and left at room temperature for at least 30 min before centrifuging at 200×g for 10 min to separate sera. Serum Osteocalcin and TRAPCP 5b level were determined by Rat Osteocalcin EIA Kit (Biomedical Technologies, Stoughton, MA) and RatTRAP™ Assay (Immunodiagnostic Systems, Scottsdale, AZ), respectively.

Colony-forming unit-fibroblast (CFU-F) and multilineage differentiation assays of bone marrow mesenchymal stem cells (MSCs)

Rats received (n=3/group) daily vehicle or PTH injections and the right tibiae were scanned by μCT as described above on day 0, 2 and 4. On day 5, the region of right tibiae corresponding to the scanned region (0–4 mm below the growth plate) and the contralateral region in left tibiae were dissected out and cut into small pieces, followed by thorough washing with αMEM. To quantify the number of MSCs, bone marrow mononuclear cells were seeded at 3×10^6/T25 flask in αMEM supplemented with 15% fetal bovine serum (FBS), 1% glutamine, 0.1% β-mercaptoethanol, 100 IU/ml penicillin and 100 μg/ml streptomycin for CFU-F assay. On day 7, the flasks were stained with 3% crystal violet in methanol and the number of CFU-F colonies, which contain more than 20 cells, were counted microscopically.

To study the osteogenic and adipogenic differentiation abilities of MSCs, bone marrow mononuclear cells were seeded at 1×10^6/well in 6-well plate and cultured for 1 week. Next, confluent cells were cultured in osteogenic medium (αMEM with 10% FBS, 10 nM dexamethasone, 10 mM β-glycerophosphate, and 50 μg/ml ascorbic acid) for 21 days followed by von Kossa staining. The plates were then scanned and quantified by ImageJ software. Alternatively, cells were cultured in adipogenic medium (αMEM with 10% FBS, 0.5 mM isobuthylmethylxanthine, 10 mM indomethacin, 1 μM dexamethasone, and 10 μg/ml insulin) for 10 days followed by Oil Red O staining. After thorough wash, the stain was dissolved in 100% isopropanol and its absorbance was measured at 500 nm.

Measurement of lipid oxidation and dead cells in bone marrow

Rats (n=3/group) received daily vehicle or PTH injections and the right tibiae were scanned by μCT as described above every other day from day 0 to 12. On day 13, 4×10^6 bone marrow mononuclear cells flushed from left and right tibiae of both groups were depleted of red blood cells, re-suspended in medium and washed with PBS. Cells were then processed to measure the amounts of malonedialdehyde (MDA), a byproduct of lipid peroxidation, using a thiobarbituric acid reactive substances (TBARS) assay kit (Cayman Chemicals, Ann Arbor, MI) according to the manufacturer's instructions. To calculate the percentage of cell death, 1×10^6 bone marrow cells were washed with PBS, stained with ethidium bromide (5 μg/ml) and acridine orange (5 μg/ml), then plated on a slide and visualized under a fluorescence microscope (Nikon Eclipse TE2000U, Nikon Instruments, Melville, NY). Cells with green color were counted as live cells and those with orange color as late apoptotic and necrotic cells [24]. For each sample, we analyzed bone marrow cells within at least 5 fields with a minimum of 500 cells per field.

Statistical Analysis

Data are expressed as means ± standard error (SEM). Longitudinal studies were analyzed by One-way ANOVA with repeated measures and nonparametric Friedman test followed by Dunns post test. Other studies were analyzed by paired and two-tailed nonparametric Wilcoxon matched-pairs signed rank test for comparison of radiated and non-radiated tibiae and by unpaired and two-tailed nonparametric Mann-Whitney test for comparison of vehicle and PTH-treated samples using Prism 5 software (GraphPad Software, San Diego, CA). The value $p<0.05$ was considered statistically significant.

Results

Radiation from multiple μCT scans has adverse effects on bone architecture

According to scanner specifications provided by the manufacturer, the radiation generated by the μCT instrument on the radiated area was 0.48 Gy per scan under the scan condition described in Material and Methods. The contralateral non-radiated legs received a negligible level of radiation during the scan. In a standard pelvic radiotherapy case, the dose to tumor is on the order of 60–72 Gy. The mean dose to the femoral heads is typically 20–30 Gy in 0.5–0.75 Gy per fraction for a total of 30–40 fractions. Thus, the radiation dose per fraction generated from μCT is in a clinically relevant range but the total dose is much lower than a typical pelvic radiotherapy patient receives.

We performed longitudinal μCT scans every other day from day 0 to day 12 on the proximal trabecular bone region of right tibiae of vehicle-treated rats (group A). As shown in Fig. 1A, compared to day 0, radiation from μCT scans led to reductions in vBMD (16%) and BV/TV (23%) starting at day 4 with more significant decreases at day 6 (26% in vBMD and 37% in BV/TV). After day 6, bone mass seemed to be stabilized and was not affected by further radiation. Analyzing structural parameters revealed that this bone loss is due to a similar

pattern of decreases in Conn.D and Tb.N* and an increase in Tb.Sp*. In addition, radiation resulted in a slight but significant increase in Tb.Th* (7.5% at day 10 and 11.3% at day 12) compared to day 0. By closely examining the 3D reconstructed trabecular bone images of radiated bone, we noticed that radiation preferentially destroyed the bone structure within the center of trabecular bone (Fig. 1B). Since the central trabeculae are thinner than those close to the cortical bone, the loss of central trabeculae could lead to an increase in Tb.Th* but this does not likely represent a true expansion of individual trabeculae. Furthermore, a significant increase in SMI starting at day 6 suggests that radiation impairs the structural integrity of trabecular bone (Fig. 1A).

Radiation is well known to have detrimental effects on the growth plate by suppressing its longitudinal growth [25]. Since μCT scanned the area just below the growth plate, we reason that the dramatic bone loss observed in the radiated area is not due to the damage on the growth plate. Indeed, the average length of radiated tibiae at day 12 (29.71±0.23 mm) was comparable to that of non-radiated contralateral tibiae (29.35±0.24 mm). The endochondral growth rate during the radiation period was calculated to be 0.420±0.002 mm/day which is consistent with a previous report [26].

Comparing the μCT data of the left tibiae between groups A and C at day 12 demonstrated that multiple μCT scans of right legs had no effect on the trabecular bone structure in left legs (Table 1), implying that focal radiation has only localized but not distal bone effects. Furthermore, within group C, we did not detect any significant difference in bone structural parameters between left and right tibiae (Table 1), suggesting that in the following experiments the non-radiated left tibiae can be used as proper controls for the radiated right tibiae.

Previous reports showed that high doses (20–50 Gy) of radiation to the entire hind limbs of rodents increases cortical BMD [11] but decreases the mechanical strength of cortical bone [11, 27, 28] and makes them prone to fractures [29]. We analyzed the cortical bone within the scanned area in group A and found no significant changes in BMD and cortical structural parameters (supplementary figure 1), which is likely due to the low dosage of radiation by μCT.

PTH treatment prevents the deterioration of trabecular bone microarchitecture caused by radiation from multiple μCT scans

In striking contrast to the bone structural damage in the radiated right tibiae of vehicle-treated rats, PTH-treated rats showed a dramatic improvement of bone microarchitecture in the radiated trabecular region (Fig. 2). vBMD was increased 27% (day 4), 30% (day 6), 45% (day 8), 61% (day 10), 81% (day 12) at a steady rate relative to baseline at day 0. Likewise, BV/TV was increased 61%, 69%, 102%, 134%, and 182% at day 4, 6, 8, 10, and 12, respectively. This enhanced bone mass was closely correlated to the continuously increased Conn.D (60%, 34%, 68%, 85%, and 137%), Tb.N* (20%, 17%, 36%, 39%, and 55%) and Tb.Th* (13%, 23%, 28%, 35%, and 43%) and reduced Tb.Sp* (17%, 16%, 29%, 30%, and 38%) during this period. SMI scores reached significant reduction at day 8 (13%),10 (20%) and 12 (28%).

On day 12, radiation from multiple μCT scans of right tibiae resulted in a great reduction of trabecular bone mass and deterioration of bone structure compared to the left tibiae (Fig. 3A). Compared to vehicle injections, 12 days of PTH injections showed dramatic anabolic actions on the non-radiated tibiae, which are consistent with previous reports [21, 30]. In a similar trend, PTH injections remarkably increased the vBMD (2.9-fold), BV/TV (4.7-fold), Conn.D (8.3-fold), Tb.N* (2.7-fold), and Tb.Th* (1.3-fold), and decreased Tb.Sp* (2.9-fold) and SMI (1.5-fold) in the radiated region compared to vehicle injections. This

radioprotective effect of PTH is so strong that there was no significant difference in bone structural parameters observed between the radiated and non-radiated tibiae in the same PTH-treated rats. Interestingly, a truncated PTH peptide (3–34), which binds to PTH1R and activates PLC/PKC pathway [31], did not rescue the radiation-induced bone loss (supplementary figure 2), suggesting a specific role of PTH1R/PKA pathway in the radioprotective effect of PTH(1–34). At the cortical site, PTH treatment significantly augmented cortical area and increased bone resistance to bending (MOI) in both radiated and non-radiated tibiae but had little effects on other cortical bone parameters (supplementary figure 1).

PTH prevents the loss of mechanical competence of whole bone segment by radiation

Whole bone stiffness measured by μFE analysis reflects the integrated mechanical competence of both cortical and trabecular compartments. Vehicle-treated non-radiated tibiae tended to have greater stiffness than the radiated tibiae ($p=0.069$, Fig. 3B). By contrast, PTH-treated non-radiated tibiae had similar stiffness as radiated tibiae ($p=0.940$). Indeed, PTH caused a significant increase in whole bone stiffness in both tibiae over 12 days. At day 12, PTH-treated radiated tibia had 71% greater stiffness than vehicle-treated radiated tibia, suggesting a significant anabolic effect in both cortical and trabecular bone compartments.

PTH rescues the radiation-induced damage on osteoblasts and MSCs

To understand the underlying mechanisms by which radiation induces bone loss and PTH rescues it, we performed bone histomorphometry on both tibiae harvested from vehicle- and PTH-treated rats at day 12. μCT-generated X-ray radiation did not change the overall marrow morphology, likely due to a low dosage (Fig. 4A). However, this radiation dosage was able to greatly suppress osteoblast number (Ob.N/BS) and osteoblast surface (Ob.S/BS) by 47% and 52%, respectively, but did not significantly affect osteoclast surface (Oc.S/BS) (Fig. 4B). In the dynamic analysis, we did not observe any calcein double-labeled surface in vehicle-treated radiated tibiae (Fig. 4C), resulting in no measurement value for mineral apposition rate (MAR) and bone formation rate (BFR). Moreover, mineral surface (MS/BS) was greatly reduced in the radiated bone (Fig. 4D). These data demonstrate that radiation strongly suppresses osteoblast differentiation and mineralization. Daily PTH injections completely reversed this adverse effect on osteoblasts. In the radiated bones, PTH dramatically increased Ob.N/BS (3.0-fold), Ob.S/BS (4.4-fold), MS/BS (2.1-fold), MAR, and BFR compared to vehicle (Fig. 4B, C, D). PTH is a potent stimulus for bone turnover. Hence, we observed that PTH increased Oc.S/BS in both tibiae about 1.6-fold compared to vehicle. It is worthwhile to note that PTH injections have similar potent effects on bone cells in radiated and non-radiated tibiae, which explain the almost identical bone structural parameters in these tibiae measured by μCT analyses. The effects of PTH on bone formation and resorption were further confirmed by elevated serum osteocalcin and TRAP levels (Fig. 4E).

Bone marrow MSCs are progenitors for osteoblasts, and bone formation in young rats requires a constant supply of osteoblasts. To elucidate the mechanism by which radiation and PTH affect osteoblast formation, we performed colony forming unit fibroblastic (CFU-F) assay to measure the number of MSCs within bone marrow. As shown in Fig. 5A, radiation greatly reduced the CFU-F colony number by 75% in the vehicle group but PTH treatment completely abrogated this effect, suggesting that PTH protects MSCs from radiation-induced damage. We further tested the multilineage differentiation abilities of these bone marrow MSCs in vitro. While both radiation and PTH had no effect on the osteogenic differentiation of these progenitors (Fig. 5B), MSCs derived from vehicle-treated radiated bones displayed more adipogenic differentiation as shown by Oil Red O staining

than non-radiated bones and PTH treatment was able to attenuate this radiation effect (Fig. 5C). Taken together, these data clearly indicate that PTH prevents radiation-induced damages and altered lineage commitment of MSCs in the bone marrow.

PTH reversed radiation-induced bone marrow cell death

Radiation causes cell death by damaging DNA and increasing free radicals, such as reactive oxygen species (ROS) [32–34]. Using a TBARS assay that measures the consequences of lipid peroxidation and MDA specifically, we found that multiple μCT scans increased the levels of free radicals in bone marrow from both vehicle and PTH-treated tibiae (Fig. 6A). However, an ethidium bromide/acridine orange staining of bone marrow cells detecting late apoptotic and necrotic cells revealed that increased free radicals resulted in augmented cell death in radiated tibiae but PTH injections were able to reduce this increase of dead cells (Fig. 6B).

Discussion

Radiation is known to cause complications in skeletal tissue and adversely affect the quality of life in cancer survivors [35]. Since radiotherapy greatly improves survivorship rate of cancer patients, it is imperative to determine how radiation affects the skeletal system and to identify a treatment to reverse its damage to bone and marrow. In the present study, we demonstrate that localized radiation generated from multiple microCT scans, which mimic the clinical fractionized radiotherapy, rapidly destroyed bone microarchitecture in young growing rats, but PTH daily injection, an anabolic treatment for osteoporosis, was able to reverse this radiation-induced bone loss. In bone, PTH1R is the only receptor for PTH and expressed in the osteoblast lineage cells, with more abundance in osteoblasts [36, 37] and osteocytes [38] than in MSCs [39]. PTH regulates the expression of many genes with a variety of functions via PTH1R. During radiation, PTH could bind to PTH1R in osteoblasts and MSCs and directly protect them from radiation-induced bone damage. Alternatively, PTH could regulate the secretion or release of certain factors from osteoblasts, osteocytes, or bone matrix and indirectly affect the survival of bone marrow cells and MSCs. More studies are required to elucidate the underlying mechanisms.

Our bone histomorphometric analyses revealed that repetitive low doses of radiation generated from μCT scans mainly suppress bone formation but have little effect on bone resorption. In bone, osteoblast lineage cells are sensitive to radiation. In vitro experiments using osteoblastic cell lines found that radiation inhibits osteoblast growth by arresting cell cycle progression, altering their differentiation ability, and sensitizing these cells toward apoptotic reagents [40–43]. Moreover, radiation destroys the osteoprogenitors, including bone marrow MSCs [44], resulting in a long-term bone loss. This radiation-induced inhibitory effect on bone formation is more prominent in the young rats used in our experiments because their trabecular bone is constantly formed through endochondral ossification derived from the growth plate. Interestingly, PTH functions in multiple pathways to increase osteoblast number and stimulate their activity. In our experiments, we demonstrated that PTH not only prevents the radiation's detrimental effects on osteoblast lineage cells but its anabolic actions on bone formation are not affected by radiation. A recent report also supports this notion that total body irradiation at a sub-lethal level on newborn mice indeed augmented the increase of bone mass induced by PTH [13]. However, in their experiments, radiation did not induce bone loss.

Previous studies presented contradictory results about the effects of radiation on osteoclasts. Some reports with total body radiation protocols revealed increased osteoclast number and surface at the early stage after radiation treatment [9, 10, 45] and further studies demonstrated that risedronate, an anti-resorptive drugs for osteoporosis, is able to prevent

this radiation-induced bone loss in mice [12]. However, several studies using localized radiation protocols suggested that radiation dramatically decreased the number of osteoclasts in bone [44, 46]. Many variables in the protocol design, such as radiation source, dosage, and time, could explain this discrepancy. One plausible reason is that total body radiation has greater systemic effects on animals, and therefore has indirect effects on osteoclast action in bone. In our study, μCT-generated localized radiation did not change total body and organ (spleen and thymus) weights (data not shown) or affect bone resorption. PTH strongly stimulates bone resorption, which is a prerequisite for bone formation during the bone remodeling process [47], regardless of radiation status. The primary event of radiation damage to bone is atrophy associated with hypocellularity and hypovascularity [48, 49]. In order to revitalize the bone tissue, we reason that anabolic drugs, such as PTH, that stimulate bone turnover to repair damaged bone matrix, are more appropriate treatments for preventing fractures in the bone surrounding the irradiated area compared to anti-resorptive drugs.

One concern for adding PTH to the radiotherapy is that radiation is a known etiologic factor for osteosarcoma [50] and that PTH treatment might further enhance the risk of osteosarcoma. Osteosarcoma is a relatively rare tumor malignancy, accounting for less than 0.2% of all cancers diagnosed annually in the US, and occurs most commonly in adolescents and young adults during growth [51]. Preclinical studies found that a significant percentage of Fisher 344 rats treated with PTH for 2 years developed osteosarcoma [52]. A subsequent dose and duration study indicated that, while a low dose (5 μg/kg/day, 3.4 times of human equivalent dose suggested by FDA) appeared to be safe, a high dose of PTH (30 μg/kg/day) for 20–24 months (70–80% of rat lifespan) resulted in osteosarcoma in 20% of rats [53]. These data eventually led to the limitation of PTH treatment to 2 years (2–3% of human lifespan) and a mandatory FDA black-box warning that “Teriparatide should not be prescribed for patients with an increased baseline risk for osteosarcoma”. However, there are only two possible cases of osteosarcoma amongst half a million osteoporosis patients treated with PTH [54], suggesting that this risk might be theoretical and negligible in humans. Indeed a 7 year US cancer surveillance study found that all patients diagnosed with adult primary osteosarcoma had no prior PTH treatment [55], thus further strengthening the hypothesis that incidences of osteosarcoma in rats may not correlate with humans. Furthermore, patients with primary or secondary hyperparathyroidism do not have increased risks of bone neoplasia [56, 57].

As an anabolic agent, PTH carries another concern for cancer patients that it might promote tumor growth. PTH(1–34) shares its receptor PTH1R with PTHrP(1–34). Since it is a 139 to 173-aa polyhormone with distinct biological functions within different regions [58], PTHrP might act on cancer cells independent of PTH1R [59]. Furthermore, while PTH daily injection executes anabolic actions on bone, continuous infusion of PTH, a mode similar to PTHrP expression in cancers, has an opposite effect with significant bone loss [60]. To date, multiple large-scale clinical trials and subsequent clinical use of teriparatide showed no evidence of increasing risks of any cancer in patients [61]. Interestingly, cancer in patients with primary hyperparathyroidism has lower mortality rates than controls [62].

There are limitations associated with this study. First, in this study we used a growing rat model, which does not mimic most of adult cancer patients receiving radiotherapy. Further studies to establish a clinically relevant focal radiation induced-bone loss model in skeletally mature rats and test whether PTH rescues this bone loss is required and these studies are currently underway in our laboratory. Second, ionizing radiation by μCT does not allow incremental dose scaling and is not a standard approach to study radiation-induced tissue damage. While its dose per fraction is in a clinically relevant range, the total radiation dosage is lower than that of a research irradiator and common radiotherapy. However,

during the irradiation procedure by μCT, high-resolution structural images of the rat skeleton can be obtained. Indeed, the in vivo imaging by μCT is one of the strengths of the current study. To our knowledge, this is the first study in which longitudinal changes in trabecular bone microarchitecture induced by radiation as well as its treatment are monitored. Such study design not only reduces animal number, but also minimizes the inter-subject variation and improves the detection of subtle bone changes. Our studies also point out that multiple in vivo scans on the same area might have adverse impacts on bone and that sufficient intervals between scans should be carefully determined to avoid such unintended effects while designing animal studies.

In summary, our study demonstrates that administration of PTH, a current drug for osteoporosis, strongly protects the bone microarchitecture from radiation-induced damage. In our focal radiation model, suppressed bone formation, due to decreased numbers and activities in MSCs and mature osteoblasts, is the major contributing factor for radiation-induced bone loss. PTH, a great stimulus for bone formation, can completely reverse these adverse effects. Though not clinically proven, the theoretical osteosarcoma and tumorigenicity concerns represent the largest hurdle of translating our findings into a clinical application. These concerns can only be addressed with future extensive pre-clinical and clinical studies.

Supplementary Material

Refer to Web version on PubMed Central for supplementary material.

Acknowledgments

We thank Dr. Laurie McCauley at the University of Michigan for her critical comments on the manuscript. This study was supported in part by pilot grant (to LQ) from Penn Center for Musculoskeletal Disorders P30AR050950 (NIAMS/NIH) and grant R25 CA101871-07 from the National Cancer Institute (to VS).

References

1. Overgaard M. Spontaneous radiation-induced rib fractures in breast cancer patients treated with postmastectomy irradiation. A clinical radiobiological analysis of the influence of fraction size and dose-response relationships on late bone damage. Acta Oncol. 1988; 27:117–122. [PubMed: 3390342]
2. Pierce SM, Recht A, Lingos TI, Abner A, Vicini F, Silver B, Herzog A, Harris JR. Long-term radiation complications following conservative surgery (CS) and radiation therapy (RT) in patients with early stage breast cancer. Int J Radiat Oncol Biol Phys. 1992; 23:915–923. [PubMed: 1639653]
3. Baxter NN, Habermann EB, Tepper JE, Durham SB, Virnig BA. Risk of pelvic fractures in older women following pelvic irradiation. Jama. 2005; 294:2587–2593. [PubMed: 16304072]
4. Elliott SP, Jarosek SL, Alanee SR, Konety BR, Dusenbery KE, Virnig BA. Three-dimensional external beam radiotherapy for prostate cancer increases the risk of hip fracture. Cancer. 2011; 117:4557–4565. [PubMed: 21412999]
5. Cummings SR, Melton LJ. Epidemiology and outcomes of osteoporotic fractures. Lancet. 2002; 359:1761–1767. [PubMed: 12049882]
6. Kanis JA, Oden A, Johnell O, De Laet C, Jonsson B, Oglesby AK. The components of excess mortality after hip fracture. Bone. 2003; 32:468–473. [PubMed: 12753862]
7. Miller CW. Survival and ambulation following hip fracture. J Bone Joint Surg Am. 1978; 60:930–934. [PubMed: 701341]
8. Cannon CP, Lin PP, Lewis VO, Yasko AW. Management of radiation-associated fractures. J Am Acad Orthop Surg. 2008; 16:541–549. [PubMed: 18768711]

9. Green DE, Adler BJ, Chan ME, Rubin CT. Devastation of adult stem cell pools by irradiation precedes collapse of trabecular bone quality and quantity. J Bone Miner Res. 2012; 27:749–759. [PubMed: 22190044]
10. Hamilton SA, Pecaut MJ, Gridley DS, Travis ND, Bandstra ER, Willey JS, Nelson GA, Bateman TA. A murine model for bone loss from therapeutic and space-relevant sources of radiation. J Appl Physiol. 2006; 101:789–793. [PubMed: 16741258]
11. Wernle JD, Damron TA, Allen MJ, Mann KA. Local irradiation alters bone morphology and increases bone fragility in a mouse model. J Biomech. 2010; 43:2738–2746. [PubMed: 20655052]
12. Willey JS, Livingston EW, Robbins ME, Bourland JD, Tirado-Lee L, Smith-Sielicki H, Bateman TA. Risedronate prevents early radiation-induced osteoporosis in mice at multiple skeletal locations. Bone. 2010; 46:101–111. [PubMed: 19747571]
13. Koh AJ, Novince CM, Li X, Wang T, Taichman RS, McCauley LK. An irradiation-altered bone marrow microenvironment impacts anabolic actions of PTH. Endocrinology. 2011; 152:4525–4536. [PubMed: 22045660]
14. Jia D, Gaddy D, Suva LJ, Corry PM. Rapid loss of bone mass and strength in mice after abdominal irradiation. Radiat Res. 2011; 176:624–635. [PubMed: 21859327]
15. Qin L, Raggatt LJ, Partridge NC. Parathyroid hormone: a double-edged sword for bone metabolism. Trends Endocrinol Metab. 2004; 15:60–65. [PubMed: 15036251]
16. Jiang Y, Zhao JJ, Mitlak BH, Wang O, Genant HK, Eriksen EF. Recombinant human parathyroid hormone (1–34) [teriparatide] improves both cortical and cancellous bone structure. J Bone Miner Res. 2003; 18:1932–1941. [PubMed: 14606504]
17. Recker RR, Bare SP, Smith SY, Varela A, Miller MA, Morris SA, Fox J. Cancellous and cortical bone architecture and turnover at the iliac crest of postmenopausal osteoporotic women treated with parathyroid hormone 1–84. Bone. 2009; 44:113–119. [PubMed: 18983947]
18. Jilka RL. Molecular and cellular mechanisms of the anabolic effect of intermittent PTH. Bone. 2007; 40:1434–1446. [PubMed: 17517365]
19. Qin, L.; Partridge, NC. Parathyroid hormone and parathyroid hormone-related protein: normal function, diseases, and emerging therapeutics. In: Bronner, F.; Farach-Carson, MC.; Roach, HI., editors. Bone-Metabolic Functions and Modulators. Springer: Topics in Bone Biology); 2012. p. 1-20.
20. Qin L, Qiu P, Wang L, Li X, Swarthout JT, Soteropoulos P, Tolias P, Partridge NC. Gene expression profiles and transcription factors involved in parathyroid hormone signaling in osteoblasts revealed by microarray and bioinformatics. J Biol Chem. 2003; 278:19723–19731. [PubMed: 12644456]
21. Li X, Liu H, Qin L, Tamasi J, Bergenstock M, Shapses S, Feyen JH, Notterman DA, Partridge NC. Determination of dual effects of parathyroid hormone on skeletal gene expression in vivo by microarray and network analysis. J Biol Chem. 2007; 282:33086–33097. [PubMed: 17690103]
22. Bouxsein ML, Boyd SK, Christiansen BA, Guldberg RE, Jepsen KJ, Muller R. Guidelines for assessment of bone microstructure in rodents using micro-computed tomography. J Bone Miner Res. 2010; 25:1468–1486. [PubMed: 20533309]
23. Parfitt AM, Drezner MK, Glorieux FH, Kanis JA, Malluche H, Meunier PJ, Ott SM, Recker RR. Bone histomorphometry: standardization of nomenclature, symbols, and units. Report of the ASBMR Histomorphometry Nomenclature Committee. J Bone Miner Res. 1987; 2:595–610. [PubMed: 3455637]
24. Ribble D, Goldstein NB, Norris DA, Shellman YG. A simple technique for quantifying apoptosis in 96-well plates. BMC Biotechnol. 2005; 5:12. [PubMed: 15885144]
25. Dawson WB. Growth impairment following radiotherapy in childhood. Clin Radiol. 1968; 19:241–256. [PubMed: 5677640]
26. Stokes IA, Aronsson DD, Dimock AN, Cortright V, Beck S. Endochondral growth in growth plates of three species at two anatomical locations modulated by mechanical compression and tension. J Orthop Res. 2006; 24:1327–1334. [PubMed: 16705695]
27. Maeda M, Bryant MH, Yamagata M, Li G, Earle JD, Chao EY. Effects of irradiation on cortical bone and their time-related changes. A biomechanical and histomorphological study. J Bone Joint Surg Am. 1988; 70:392–399. [PubMed: 3346264]

28. Sugimoto M, Takahashi S, Toguchida J, Kotoura Y, Shibamoto Y, Yamamuro T. Changes in bone after high-dose irradiation. Biomechanics and histomorphology. J Bone Joint Surg Br. 1991; 73:492–497. [PubMed: 1670456]
29. Damek-Poprawa M, Both S, Wright AC, Maity A, Akintoye SO. Onset of mandible and tibia osteoradionecrosis: a comparative pilot study in the rat. Oral Surg Oral Med Oral Pathol Oral Radiol. 2013; 115:201–211. [PubMed: 23254371]
30. Hock JM, Fonseca J, Gunness-Hey M, Kemp BE, Martin TJ. Comparison of the anabolic effects of synthetic parathyroid hormone-related protein (PTHrP) 1–34 and PTH 1–34 on bone in rats. Endocrinology. 1989; 125:2022–2027. [PubMed: 2791976]
31. Fujimori A, Cheng SL, Avioli LV, Civitelli R. Structure-function relationship of parathyroid hormone: activation of phospholipase-C, protein kinase-A and -C in osteosarcoma cells. Endocrinology. 1992; 130:29–36. [PubMed: 1727705]
32. Hall, EJ. Radiobiology for the radiologist. Philadelphia, PA: Lippincott Williams & Wilkins; 2000.
33. Bauer G. Low dose radiation and intercellular induction of apoptosis: potential implications for the control of oncogenesis. Int J Radiat Biol. 2007; 83:873–888. [PubMed: 18058371]
34. Cooke MS, Evans MD, Dizdaroglu M, Lunec J. Oxidative DNA damage: mechanisms, mutation, and disease. FASEB J. 2003; 17:1195–1214. [PubMed: 12832285]
35. Aksnes LH, Bruland OS. Some musculo-skeletal sequelae in cancer survivors. Acta Oncol. 2007; 46:490–496. [PubMed: 17497316]
36. Fermor B, Skerry TM. PTH/PTHrP receptor expression on osteoblasts and osteocytes but not resorbing bone surfaces in growing rats. J Bone Miner Res. 1995; 10:1935–1943. [PubMed: 8619374]
37. Rouleau MF, Mitchell J, Goltzman D. In vivo distribution of parathyroid hormone receptors in bone: evidence that a predominant osseous target cell is not the mature osteoblast. Endocrinology. 1988; 123:187–191. [PubMed: 2838253]
38. Bellido T, Saini V, Pajevic PD. Effects of PTH on osteocyte function. Bone. 2012; 24:01245–01248.
39. Mendez-Ferrer S, Michurina TV, Ferraro F, Mazloom AR, Macarthur BD, Lira SA, Scadden DT, Ma'ayan A, Enikolopov GN, Frenette PS. Mesenchymal and haematopoietic stem cells form a unique bone marrow niche. Nature. 2010; 466:829–834. [PubMed: 20703299]
40. Dudziak ME, Saadeh PB, Mehrara BJ, Steinbrech DS, Greenwald JA, Gittes GK, Longaker MT. The effects of ionizing radiation on osteoblast-like cells in vitro. Plast Reconstr Surg. 2000; 106:1049–1061. [PubMed: 11039376]
41. Gal TJ, Munoz-Antonia T, Muro-Cacho CA, Klotch DW. Radiation effects on osteoblasts in vitro: a potential role in osteoradionecrosis. Arch Otolaryngol Head Neck Surg. 2000; 126:1124–1128. [PubMed: 10979127]
42. Matsumura S, Jikko A, Hiranuma H, Deguchi A, Fuchihata H. Effect of X-ray irradiation on proliferation and differentiation of osteoblast. Calcif Tissue Int. 1996; 59:307–308. [PubMed: 8781058]
43. Szymczyk KH, Shapiro IM, Adams CS. Ionizing radiation sensitizes bone cells to apoptosis. Bone. 2004; 34:148–156. [PubMed: 14751572]
44. Cao X, Wu X, Frassica D, Yu B, Pang L, Xian L, Wan M, Lei W, Armour M, Tryggestad E, Wong J, Wen CY, Lu WW, Frassica FJ. Irradiation induces bone injury by damaging bone marrow microenvironment for stem cells. Proc Natl Acad Sci U S A. 2011; 108:1609–1614. [PubMed: 21220327]
45. Kondo H, Yumoto K, Alwood JS, Mojarrab R, Wang A, Almeida EA, Searby ND, Limoli CL, Globus RK. Oxidative stress and gamma radiation-induced cancellous bone loss with musculoskeletal disuse. J Appl Physiol. 2009; 108:152–161. [PubMed: 19875718]
46. Sawajiri M, Mizoe J, Tanimoto K. Changes in osteoclasts after irradiation with carbon ion particles. Radiat Environ Biophys. 2003; 42:219–223. [PubMed: 13680258]
47. Wu X, Pang L, Lei W, Lu W, Li J, Li Z, Frassica FJ, Chen X, Wan M, Cao X. Inhibition of Sca-1-positive skeletal stem cell recruitment by alendronate blunts the anabolic effects of parathyroid hormone on bone remodeling. Cell Stem Cell. 2010; 7:571–580. [PubMed: 21040899]

48. Howland WJ, Loeffler RK, Starchman DE, Johnson RG. Postirradiation atrophic changes of bone and related complications. Radiology. 1975; 117:677–685. [PubMed: 1188119]
49. Ergun H, Howland WJ. Postradiation atrophy of mature bone. CRC Crit Rev Diagn Imaging. 1980; 12:225–243. [PubMed: 6985580]
50. Ottaviani G, Jaffe N. The etiology of osteosarcoma. Cancer Treat Res. 2009; 152:15–32. [PubMed: 20213384]
51. Jemal A, Siegel R, Ward E, Murray T, Xu J, Thun MJ. Cancer statistics, 2007. CA Cancer J Clin. 2007; 57:43–66. [PubMed: 17237035]
52. Vahle JL, Sato M, Long GG, Young JK, Francis PC, Engelhardt JA, Westmore MS, Linda Y, Nold JB. Skeletal changes in rats given daily subcutaneous injections of recombinant human parathyroid hormone (1–34) for 2 years and relevance to human safety. Toxicol Pathol. 2002; 30:312–321. [PubMed: 12051548]
53. Vahle JL, Long GG, Sandusky G, Westmore M, Ma YL, Sato M. Bone neoplasms in F344 rats given teriparatide [rhPTH(1–34)] are dependent on duration of treatment and dose. Toxicol Pathol. 2004; 32:426–438. [PubMed: 15204966]
54. Subbiah V, Madsen VS, Raymond AK, Benjamin RS, Ludwig JA. Of mice and men: divergent risks of teriparatide-induced osteosarcoma. Osteoporos Int. 2010; 21:1041–1045. [PubMed: 19597911]
55. Andrews EB, Gilsenan AW, Midkiff K, Sherrill B, Wu Y, Mann BH, Masica D. The US postmarketing surveillance study of adult osteosarcoma and teriparatide: Study design and findings from the first 7 years. J Bone Miner Res. 2012; 18
56. Jimenez C, Yang Y, Kim HW, Al-Sagier F, Berry DA, El-Naggar AK, Patel S, Vassilopoulou-Sellin R, Gagel RF. Primary hyperparathyroidism and osteosarcoma: examination of a large cohort identifies three cases of fibroblastic osteosarcoma. J Bone Miner Res. 2005; 20:1562–1568. [PubMed: 16059628]
57. Tashjian AH Jr, Chabner BA. Commentary on clinical safety of recombinant human parathyroid hormone 1–34 in the treatment of osteoporosis in men and postmenopausal women. J Bone Miner Res. 2002; 17:1151–1161. [PubMed: 12096828]
58. Philbrick WM, Wysolmerski JJ, Galbraith S, Holt E, Orloff JJ, Yang KH, Vasavada RC, Weir EC, Broadus AE, Stewart AF. Defining the roles of parathyroid hormone-related protein in normal physiology. Physiol Rev. 1996; 76:127–173. [PubMed: 8592727]
59. Park SI, McCauley LK. Nuclear localization of parathyroid hormone-related peptide confers resistance to anoikis in prostate cancer cells. Endocr Relat Cancer. 2012; 19:243–254. [PubMed: 22291434]
60. Tam CS, Heersche JN, Murray TM, Parsons JA. Parathyroid hormone stimulates the bone apposition rate independently of its resorptive action: differential effects of intermittent and continuous administration. Endocrinology. 1982; 110:506–512. [PubMed: 7056211]
61. File E, Deal C. Clinical update on teriparatide. Curr Rheumatol Rep. 2009; 11:169–176. [PubMed: 19604460]
62. Wermers RA, Khosla S, Atkinson EJ, Grant CS, Hodgson SF, O'Fallon WM, Melton LJ 3rd. Survival after the diagnosis of hyperparathyroidism: a population-based study. Am J Med. 1998; 104:115–122. [PubMed: 9528728]

Highlights

- Focal radiation of the right tibiae in young rats by micro-CT severely decreases trabecular bone mass and deteriorates bone structure.
- PTH daily injections remarkably improve trabecular bone structure and strength in both radiated and non-radiated tibiae.
- Radiation damages osteoblasts and their progenitors and PTH is able to reverse these adverse effects.
- PTH protects bone marrow cells from radiation-induced cell death.
- Our data demonstrate a radioprotective effect of PTH on bone structure and bone marrow.

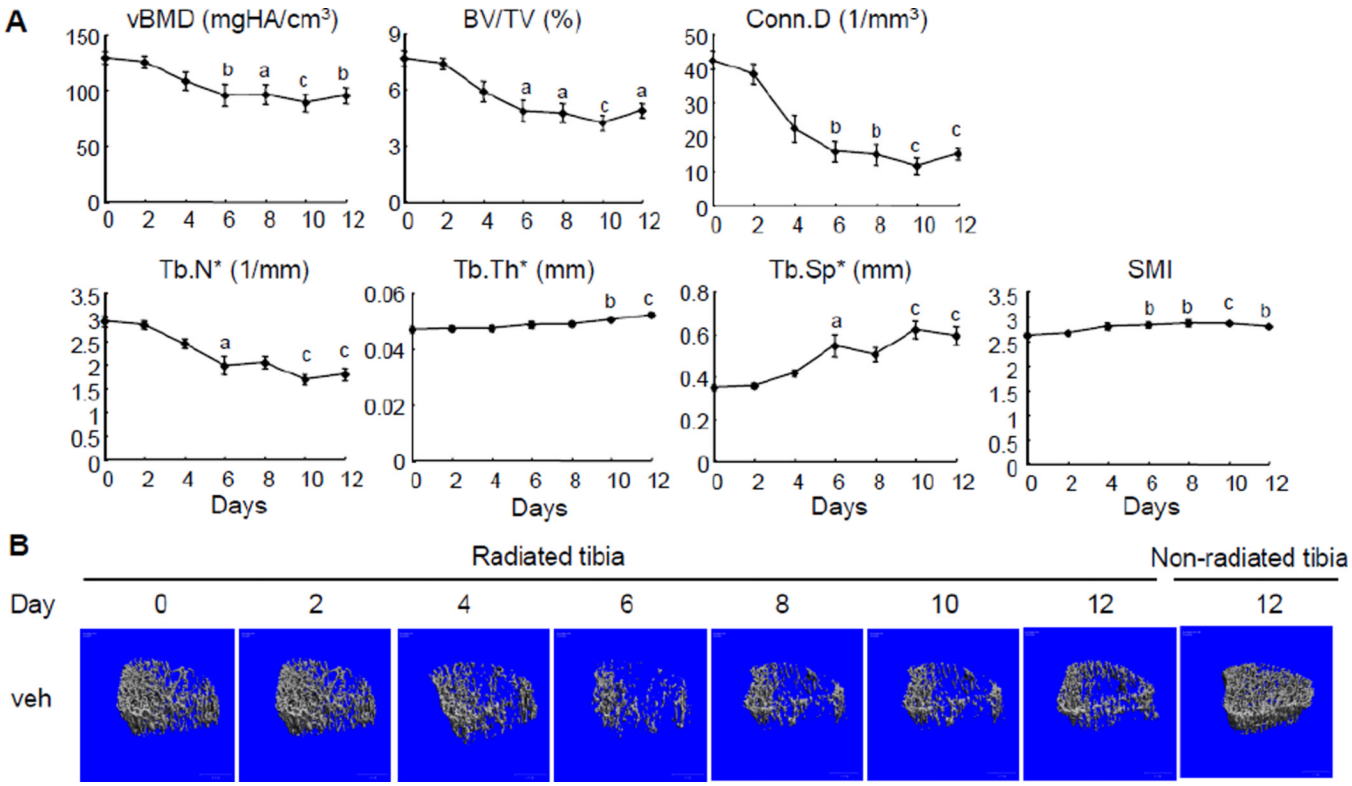

Figure 1.

Radiation from multiple μCT scans damages trabecular bone architecture in young rats. (A) Longitudinal μCT measurement of bone structural parameters in the proximal trabecular area of right tibiae from vehicle-treated rats. a; $p<0.05$; b: $p<0.01$; c: $p<0.001$ vs day 0. (B) Representative μCT images of the proximal trabecular bone of the same right (radiated) tibia of a vehicle-treated rat on day 0, 2, 4, 6, 8, 10, and 12 and the corresponding region of the left (non-radiated) tibia on day 12.

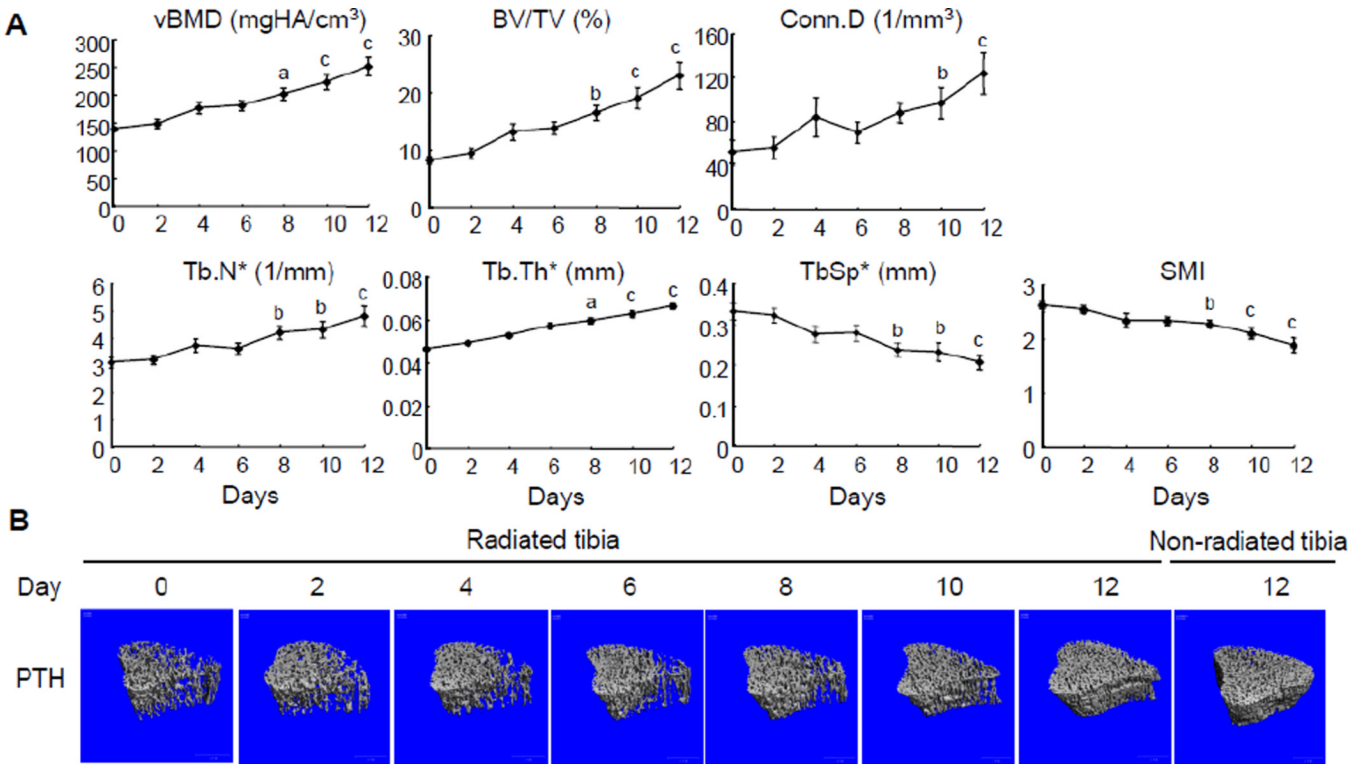

Figure 2.

PTH injections greatly improve the trabecular bone architecture regardless of radiation from multiple μCT scans.

(A) Longitudinal μCT measurement of bone structural parameters in the proximal trabecular area of right tibiae from rats injected with PTH daily. a; $p<0.05$; b: $p<0.01$; c: $p<0.001$ vs day 0.

(B) Representative μCT images of the proximal trabecular bone of the same right tibia of a PTH-treated rat on day 0, 2, 4, 6, 8, 10, and 12 and the corresponding region of the left tibia on day 12.

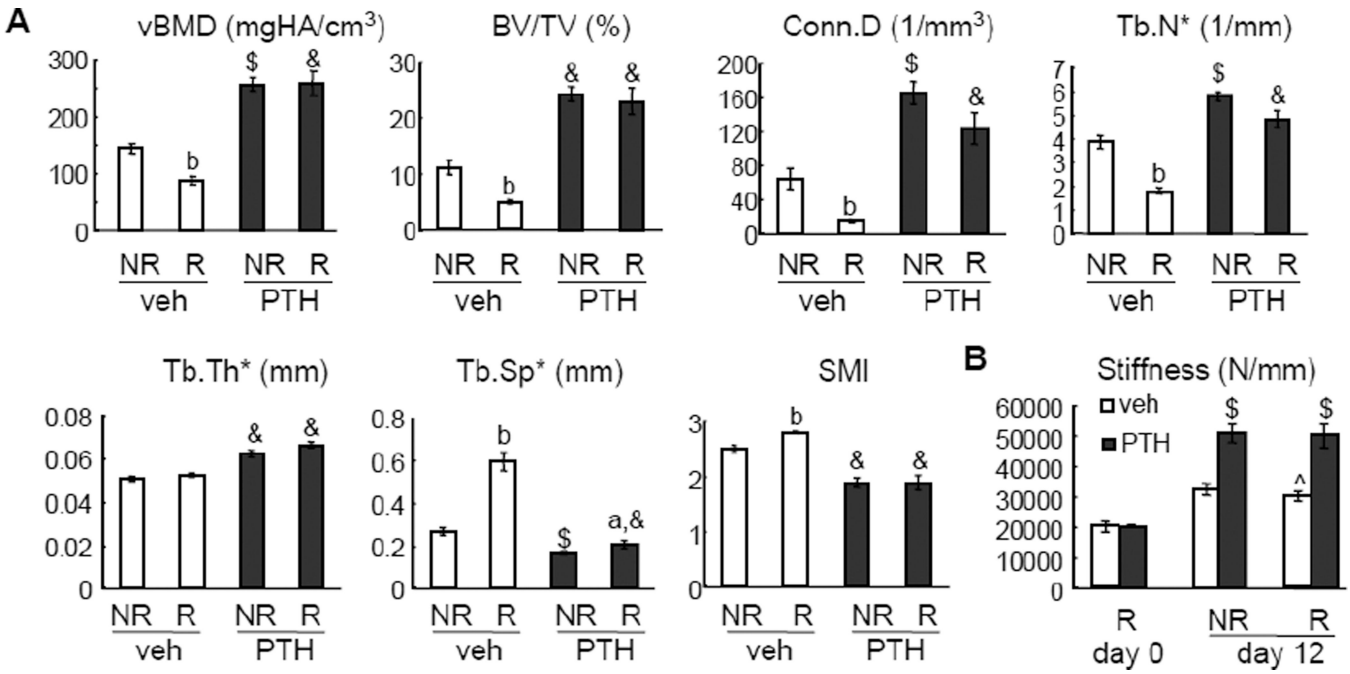

Figure 3.

PTH reverses radiation-induced bone loss and damage.

(A) μCT measurement of bone structural parameters in the proximal trabecular area of both left (non-radiated, NR) and right (radiated, R) tibiae from either vehicle- or PTH-treated rats at day 12.

(B) Whole bone stiffness measured by μFE analysis at day 0 and 12.

a: $p<0.05$; b: $p<0.01$ R vs NR; $: $p<0.01$; &: $p<0.001$ PTH vs veh; ^: $p=0.069$ vs veh NR at day 12.

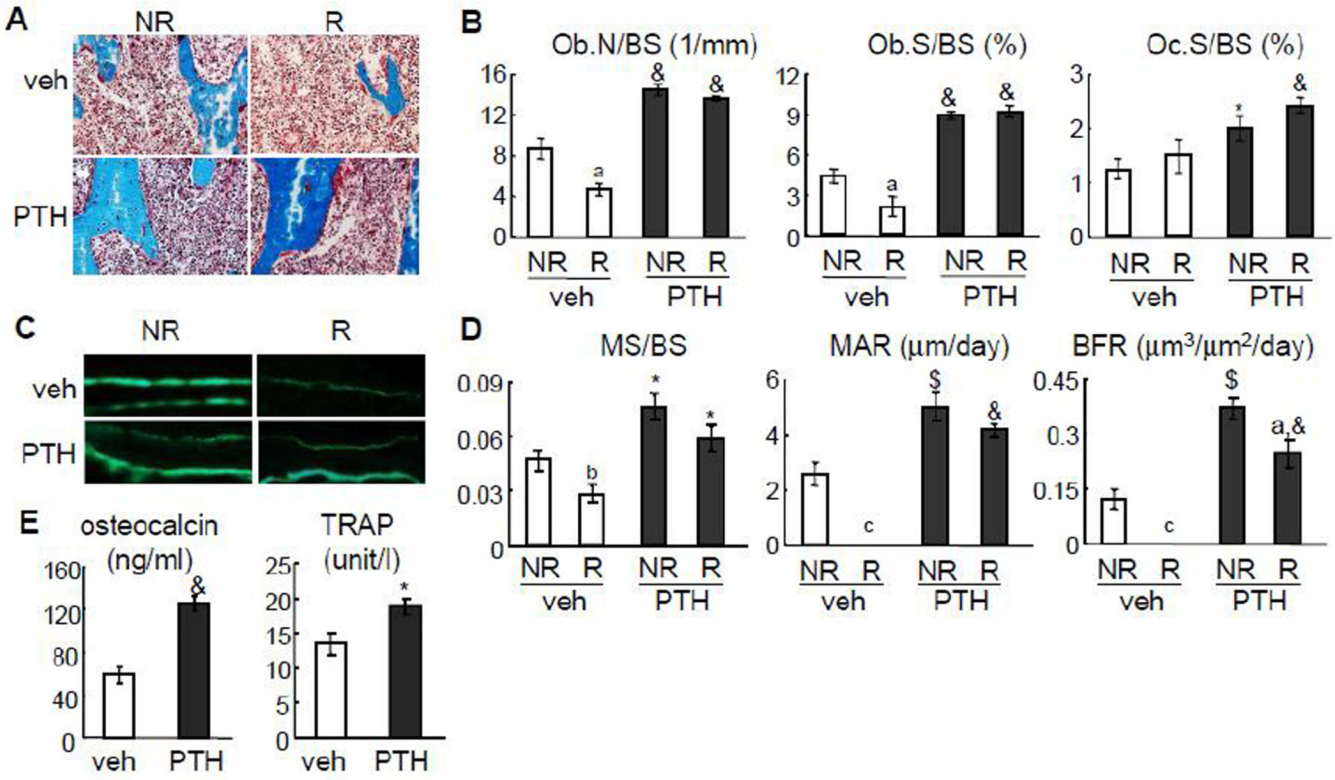

Figure 4.

PTH injections prevent radiation-induced damage on osteoblasts.

(A) Goldner's trichrome staining of trabecular bone sections from left and right tibiae of vehicle- and PTH-treated rats.

(B) Static bone histomorphometry analysis of proximal trabecular area of both left (NR) and right (R) tibiae from either vehicle- or PTH-treated rats at day 12.

(C) Representative calcein double labeling in the trabecular bone from left and right tibiae of vehicle- and PTH-treated rats.

(D) Dynamic bone histomorphometry analysis of proximal trabecular area of both left (NR) and right (R) tibiae from either vehicle- or PTH-treated rats at day 12.

(E) ELISA analyses of serum concentrations of bone formation (osteocalcin) and resorption (TRAP) markers after 12 days of PTH injections.

a: $p<0.05$; b: $p<0.01$; c: $p<0.001$ R vs NR; *: $p<0.05$; $: $p<0.01$; &: $p<0.001$ PTH vs veh.

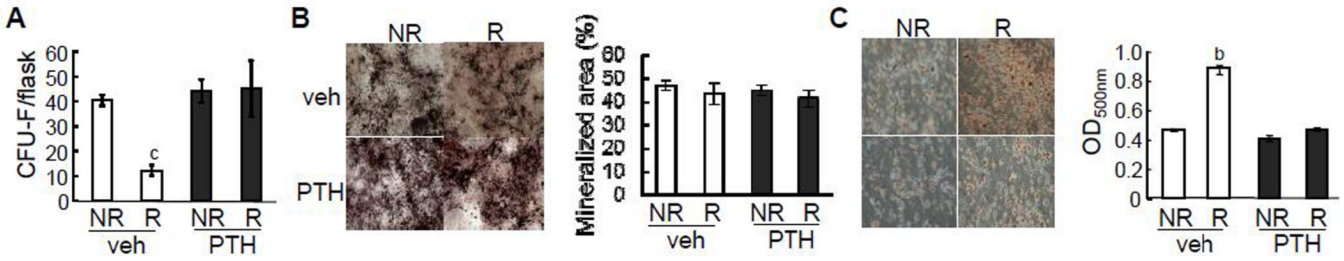

Figure 5.

PTH injections prevent radiation-induced damage on MSCs.

(A) CFU-F assays of bone marrow cells harvested from the radiated and contralateral regions in vehicle- and PTH-treated rats.

(B,C) Osteogenic (B) and adipogenic (C) differentiation assays of bone marrow MSCs derived from the radiated and contralateral regions in vehicle- and PTH-treated rats. The quantification of staining was shown on the right panel.

b: $p<0.01$; c: $p<0.001$ R vs NR.

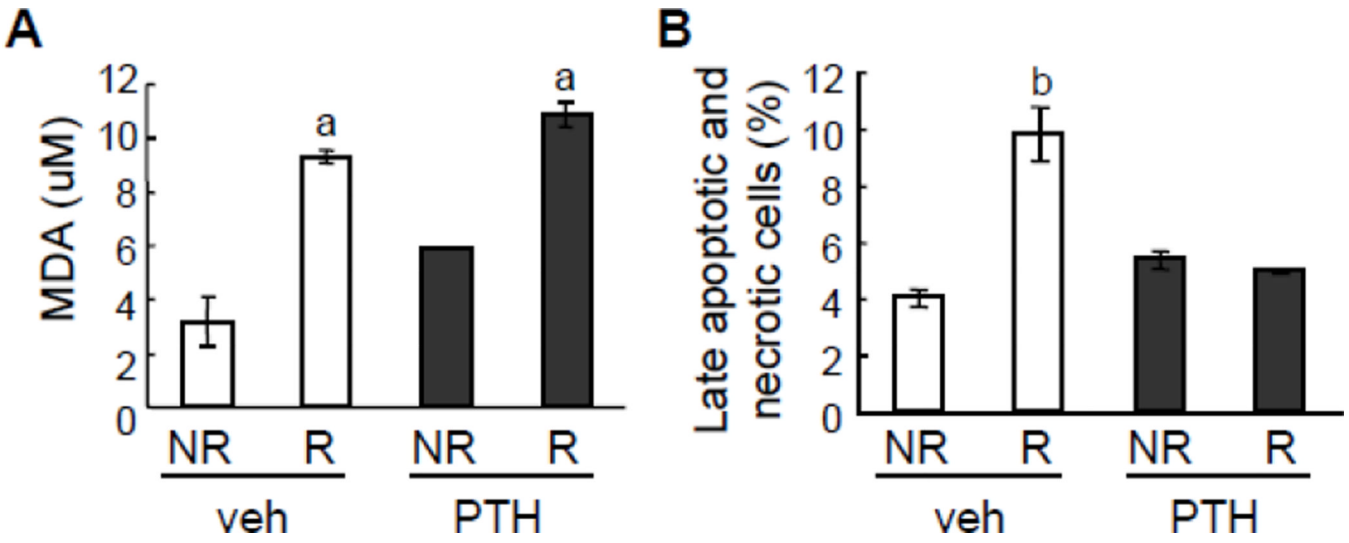

Figure 6.

PTH does not prevent radiation-induced ROS formation but abrogates radiation-induced cell death in bone marrow.

Bone marrow cells collected from radiated and non-radiated tibiae of rats treated with either vehicle or PTH were processed for measuring MDA amount (A) and ethidium bromide/ acridine orange staining to quantify dead cells (B). a: $p<0.05$; b: $p<0.01$ R vs NR.

Table 1

Trabecular bone parameters of proximal left tibiae in vehicle-treated (group A) and proximal left and right tibiae in control (group C) rats measured by μCT.

	Group A	Group C	
	Left tibiae	**Left tibiae**	**Right tibiae**
vBMD (mgHA/cm^3)	143.2±8.5	147.2±11.4	130.3±11.4
BV/TV (%)	9.20±0.72	9.82±1.19	8.63±1.16
Conn.D (1/mm^3)	46.76±5.82	60.74±12.72	43.25±9.97
Tb.N* (1/mm)	3.45±0.13	3.79±0.33	3.41±0.30
Tb.Sp* (mm)	0.290±0.010	0.273±0.026	0.298±0.031
Tb.Th* (mm)	0.049±0.001	0.047±0.001	0.047±0.001
SMI	2.57±0.05	2.56±0.08	2.59±0.09